

# Creation of high-fluence precursors by 351-nm laser exposure on SiO<sub>2</sub> substrates

David A. Cross\* and Christopher Wren Carr

Lawrence Livermore National Laboratory, Livermore, California, United States

**Abstract.** The onset of laser-induced damage on the exit surface of fused silica optics when exposed to UV ns pulses is a limiting factor in the design and operation of most high-energy laser systems. As such, significant effort has been expended in developing laser damage testing protocols and procedures to inform laser system design and operating limits. These tests typically rely on multiple laser exposures for statistical validation. For large aperture systems, testing an area equal to that of the optical components in the system is functionally impossible; instead, sub-scale witness samples are interrogated with elevated fluences. We show that, under certain circumstances, the laser exposure used to test one location on a sample will generate additional, laser-induced damage precursors in regions beyond that exposed to laser light and hence degrade the damage performance observed on subsequent exposures. We hypothesize the precursors result from condensation of vaporized silica, which re-condenses as SiO<sub>x</sub> particles deposited on the exit surface. In addition, we will outline the conditions under which this phenomenon occurs, as well as methods for mitigating or eliminating the effect. © 2020 Society of Photo-Optical Instrumentation Engineers (SPIE) [DOI: [10.1117/1.OE.60.3.031010](https://doi.org/10.1117/1.OE.60.3.031010)]

**Keywords:** laser damage; SiO<sub>2</sub>; fused silica; raster; damage test.

Paper 20201215SS received Oct. 12, 2020; accepted for publication Dec. 11, 2020; published online Dec. 29, 2020.

## 1 Introduction

Increased demand for damage-resistant optics is driven by high-power laser systems, such as National Ignition Facility, Laser Mégajoule, and Shenguang-III. There has been significant effort put into improving the manufacture, polish, and surface treatment of fused silica optics in order to increase their laser damage performance, specifically for exposure to UV laser irradiation. This effort has been tremendously successful over the last 20 years; the fluence required for the onset of laser damage has increased by more than an order of magnitude (Fig. 1).<sup>1-5</sup>

Central to the success of increased damage performance is the ability to evaluate how changes in fabrication methods affect surface quality. As surface qualities have improved, the requirements for damage testing have also evolved. Exit surface damage testing performed in the mid 90s often used 3-ns Gaussian equivalent UV fluences in the 3-J/cm<sup>2</sup> range<sup>6</sup> while testing today routinely exposes modern samples to fluences in excess of 40 J/cm<sup>2</sup>. This increase in the required fluence for damage testing on fused silica optics has resulted in increased complexity of the measurements and analysis of data collected from these damage tests. One example of this increase in complexity is the creation of a new class of laser-generated high-fluence damage precursors described in this work.

## 2 Experimental

The tests described in this work are primarily conducted in the Optical Science Laser (OSL) facility, which is described elsewhere.<sup>7</sup> The OSL Nd:glass laser, capable of outputting 300 J of 1053-nm ( $1\omega$ ) light that is frequency tripled to 351 nm ( $3\omega$ ) using a potassium dihydrogen phosphate second-harmonic generator and a potassium dideuterium phosphate third-harmonic generator, can deliver 100 J of  $3\omega$  light in a nominally flat top 5-ns temporal profile and spatial

---

\*Address all correspondence to David A. Cross, [cross22@llnl.gov](mailto:cross22@llnl.gov)

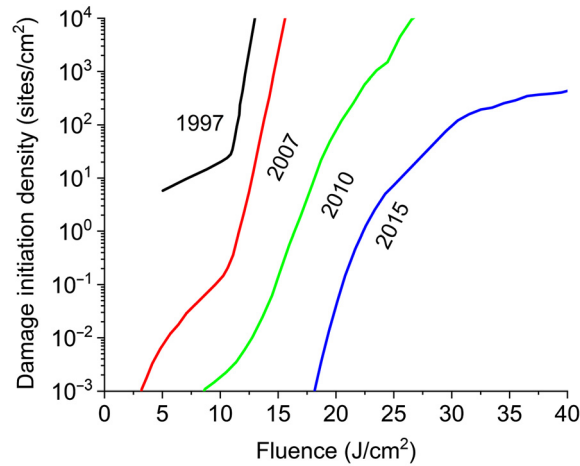


**Fig. 1** Damage performance of silica surfaces over the last 20 years.<sup>1</sup>

profile with either a 1- or 3-cm-diameter spot. The experiments described in this work are conducted on 5-cm-diameter, 1-cm-thick fused silica substrates, which have undergone high-precision polish, and a post-polish etch surface treatment resulting in common exit surface damage onset fluences in the 30-J/cm<sup>2</sup> range.<sup>1</sup>

The primary damage test in this work is the  $\rho(\phi)$  measurement, which is accomplished by simultaneously exposing  $\sim 1$  cm<sup>2</sup> on a sample, which is held at a vacuum of  $\sim 10^{-6}$  torr, with a laser beam which has local variations in the fluence. This allows a range of fluences to be tested with a single laser exposure. After a laser exposure, the tested region is scanned on a microscope, which records size, number, and location of every damage site initiated. This data can be registered to the spatial profile of the laser beam by use of engineered fiducials on the sample and in the laser beam. This technique allows each damage site to be assigned the local fluence with which it was initiated. Binning data over all regions with similar fluence provides a total area exposed and the number of damage sites initiated at a specific fluence. Repeating the analysis in discrete fluence steps generates a data set of initiated damage site density versus initiating fluence; we refer to this as  $\rho(\phi)$ .<sup>8</sup>

We used this technique to measure five independent regions on a sample, arranged as shown in Fig. 2 all with nominally identical laser exposures of 34 J/cm<sup>2</sup>  $3\omega$ , 5-ns flat-in-time (FIT) pulses.

Figures 3(a) and 3(b) show micrographs of the first and fifth region exposed, respectively. When all five exposures are analyzed by the  $\rho(\phi)$  method, the quantitative results were fit using an exponential (seen in Fig. 4) revealing the systematic increase in damage density in regions 1 through region 5. We hypothesize that this change in damage performance is the result of the creation of additional damage precursors on each sequential exposure. Moreover, these precursors are distributed across the sample even in regions, which have not been exposed to laser fluence.



**Fig. 2** Sample layout of a typical 2-in. silica sample used for  $\rho(\phi)$  damage testing.

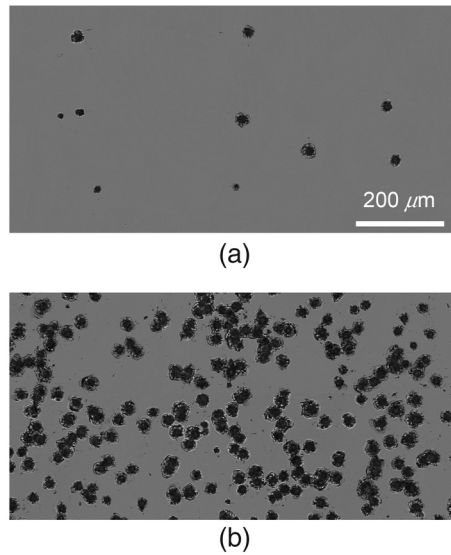


**Fig. 3** Microscopy of different laser exposure regions under identical laser conditions (a) after first exposure and (b) after fifth exposure.

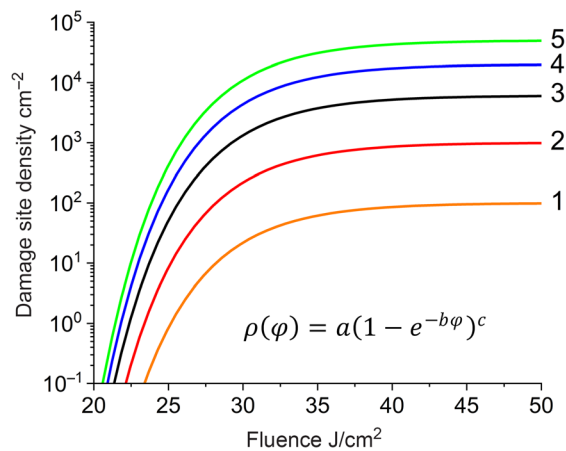


**Fig. 4** Best-fit lines for  $\rho(\phi)$  damage results for exposure regions 1 through 5 on a 2-in. silica sample. Each region was exposed only a single time in an order indicated by the region number.

It is not necessary to damage the sample in order to produce these precursors. The silica sample displayed in Fig. 5(a) was first exposed three times with 12-J/cm<sup>2</sup> laser pulses. This region was examined under optical microscopy, and no classical laser damage was observed. In fact, no modification of the surface of any kind was observed with a resolution of 1 μm. Next, this sample and a control sample seen in Fig. 5(b) were exposed to 5-ns FIT pulses with average fluences of 34 J/cm<sup>2</sup> and  $\rho(\phi)$  measured. The difference in damage performance can be seen qualitatively in Fig. 5 and the  $\rho(\phi)$  results, which quantify the change in damage performance, can be seen in Fig. 6. It has been well-studied that contamination from sources including laser-induced damage can have a dramatic effect on the laser damage performance of an optic.<sup>9,10</sup> In this situation, however, the lack of classical damage initiation by the 12-J/cm<sup>2</sup> fluence exposures shows that these precursors are not molten or fractured material from classical damage sites as no such damage is required for their generation. This leads us to the hypothesis that the precursors consist of vaporized surface material from the “undamaged” regions. In addition, the precursors are not observed to damage at 3ω, 5-ns FIT fluences below about 20 J/cm<sup>2</sup>.

In addition to the evaluation of damage site density, the effect of these high-fluence precursors on damage site size was also studied. It has been shown that average damage site diameter is

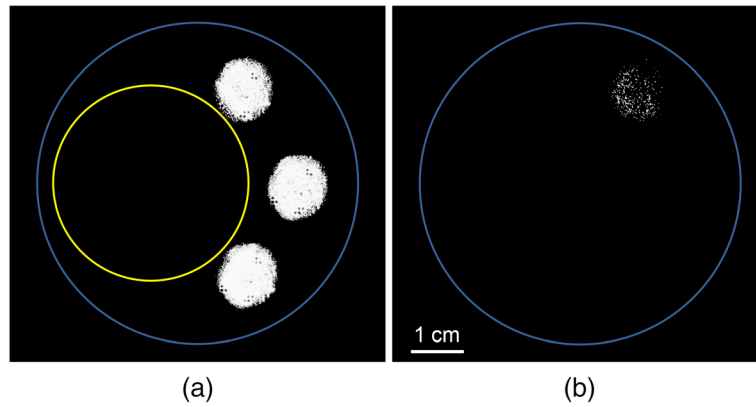


**Fig. 5** Light scatter images of damage created on (a) a sample pre-exposed with 12 J/cm<sup>2</sup> in the noted region and (b) a control sample without pre-exposure.

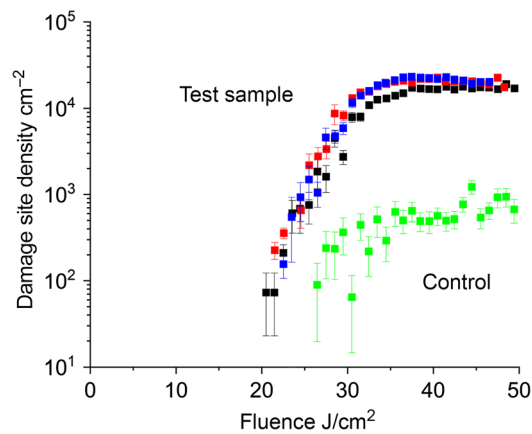


**Fig. 6**  $\rho(\phi)$  data collected from the sample pre-exposed with a large aperture and from the control sample.

linearly dependent on fluence and strongly dependent on pulse duration for flat in time pulses.<sup>11</sup> The impact of the high-fluence precursors on damage site diameter was studied by comparing the mean damage site diameter as a function of laser fluence for both pristine and degraded surfaces. As seen in Fig. 7, the average size of damage sites on the control sample and pre-exposed (degraded) sample are similar at low fluences, but the diameter of sites is larger on the degraded sample at higher fluences. This is consistent with the lower initiation fluence required for these high-fluence precursors as more of the pulse is available to grow the site.<sup>12</sup>

During this investigation of damage site size dependence, the effect of high-fluence precursors generated by different temporal pulse configurations was also tested. To probe the time scale of precursor generation, a more complex temporal pulse shape was tested. Two 2.5-ns FIT pulses were applied in quick succession with only a 10-ns gap between them. As can be seen in Fig. 8, the damage site density initiated by the double 2.5-ns pulse displayed the same systematic degradation with successive laser exposures. The damage site diameter for the sites initiated by the double pulse are significantly larger than those initiated by the single pulse (Figs. 8 and 9); this  $\sim 3\times$  increase in diameter is expected as the increased absorbed energy allows for the initiated sites to grow larger during their initiation.<sup>13</sup> In addition, the lack of a bimodal distribution of damage site sizes with the double pulse compared to the single leads us to the conclusion that the generation of these precursors on the surface occurs on time scales longer than 10 ns.

To eliminate the possibility that these high-fluence precursors were unique to large-aperture laser exposure, an experiment was performed in which two samples were each exposed to a small beam raster. The small beam raster technique has been used historically for various purposes

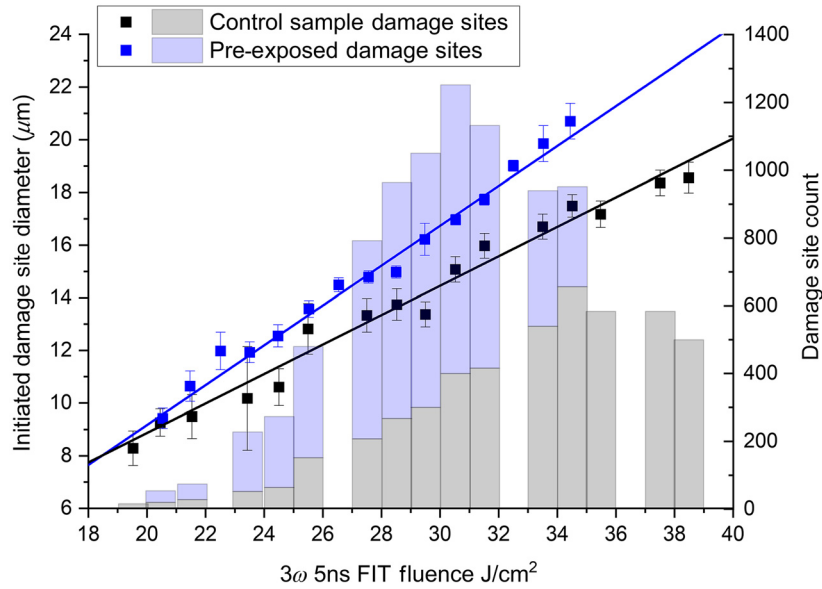


**Fig. 7** Number of damage sites (bars) and mean damage site size (points) as a function of laser fluence for both a degraded and pristine sample.

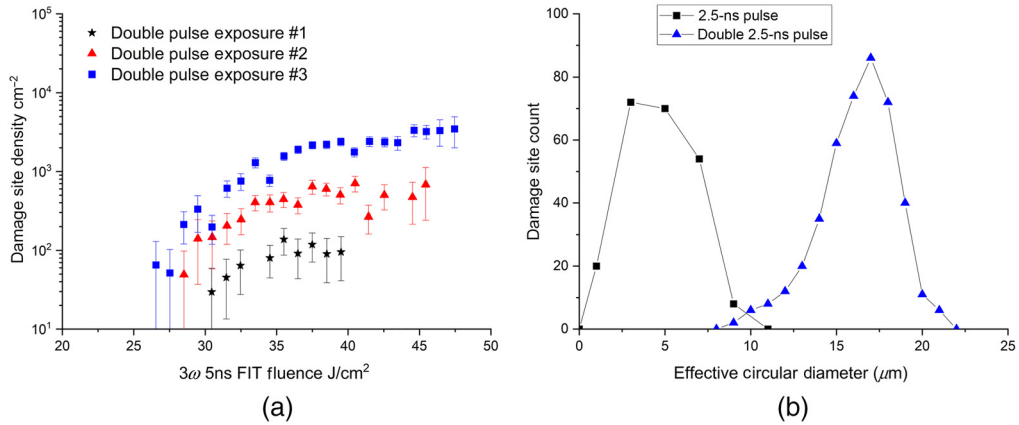


**Fig. 8** (a) The initiated damage density and (b) the damage site size distribution for damage sites initiated by single and double 2.5-ns pulses.

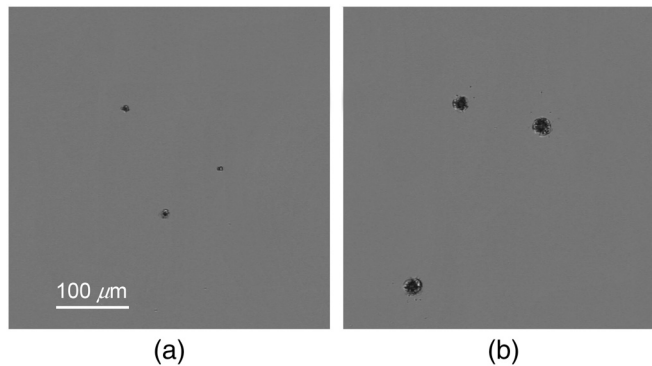


**Fig. 9** Microscopy of damage sites initiated by (a) a single 2.5-ns pulse and (b) a double 2.5-ns pulse.

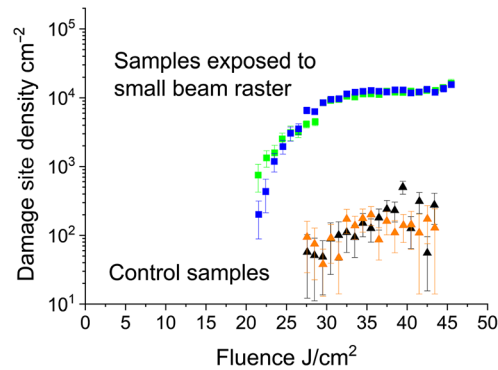


**Fig. 10**  $\rho(\phi)$  data collected from the sample pre-exposed with a small beam raster and from the control sample.

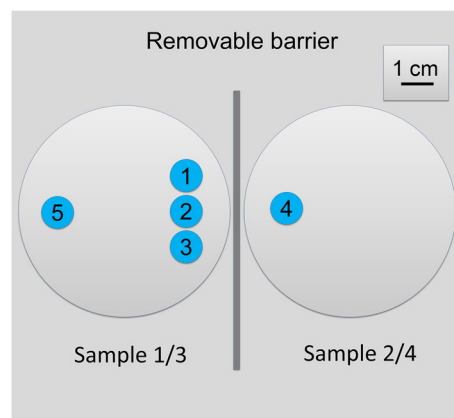


**Fig. 11** Sample layout showing two samples side by side and the order of laser exposure. The barrier shown was installed for samples 3 and 4 but not 1 and 2.

including laser damage testing due to the relatively low laser power requirements and ease of testing.<sup>14–16</sup> This raster consisted of 300 individual sites with 650- $\mu\text{m}$  spacing on each sample. Each individual exposure consisted of a single 351-nm, 80-mJ, 7-ns Gaussian laser pulse Gaussian spot with a  $1/e^2$  width of 600  $\mu\text{m}$ . This type of small beam exposure is ubiquitous in laser damage studies.<sup>6,17–19</sup> After exposure with the raster, these two samples, along with two control samples, were then individually exposed to  $\rho(\phi)$  testing to evaluate the impact of the raster on damage performance. The results of these tests can be seen in Fig. 10, and again clearly indicate a significant increase in damage site density at a given fluence compared to the control samples.

To better define the nature of the precursors and their mobility, a series of experiments was planned in which two samples are held in close proximity during a series of laser pulses. Various barriers were prepared to restrict precursor transport between the two samples (Fig. 11). In the first (control) experiment, no barrier was used. Five regions (four on one sample and one on the other) were sequentially exposed to a 5-ns FIT 34-J/cm<sup>2</sup> laser pulse. The damage density induced with 34 J/cm<sup>2</sup> is normalized to the value observed in region 1 and the progression for each subsequent region is plotted in Fig. 12. The steady rate of increase in damage site density regardless of which sample was exposed indicates that the precursors are not limited to a single surface and are particulate in nature. In a second experiment, a 50-mm-long, 25-mm-tall barrier is introduced between the two new samples (samples 3 and 4) and the shot sequence repeated. The normalized damage density seen in Fig. 12 for this shot sequence indicates that, within measurement error, the barrier completely prevents transfer of the precursors between samples.

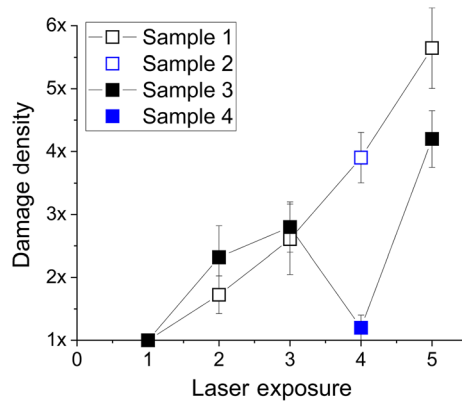


**Fig. 12** Damage density for a given fluence for the two-sample experiment. Samples 1 and 2 did not include a barrier while samples 3 and 4 did.

### 3 Analysis

We hypothesize that, when SiO<sub>2</sub> is exposed to 351-nm laser light, substrate material is vaporized and ejected from the surface.<sup>20</sup> This material condenses into nanoparticles which can redeposit on the surface outside the region exposed to the laser light. These nanoparticles are aided in redeposition due to an induced charge differential between the particles and the substrate.<sup>21</sup> When these nanoparticles redeposit on the surface, they act as damage precursors for subsequent laser exposures resulting in a systematic decrease in damage performance.<sup>22,23</sup> The efficacy of the physical barrier in blocking redeposition indicates the trajectory of these nanoparticles is shallow and line of sight.

The effect of these high-fluence precursors can be circumvented by several methods. First, the introduction of a physical barrier can be used to block the trajectories of the nanoparticles, preventing deposition of the high-fluence precursors. Second, the precursors generated in this method have only been observed to damage at fluences above 20 J/cm<sup>2</sup>. By limiting the fluence of all subsequent laser exposures to fluences below this threshold, the damaging effects of these precursors can be mitigated, if not avoided outright. It should be noted that these precursors are still being generated even at fluences as low as 12 J/cm<sup>2</sup>. Finally, it has been shown that these precursors can be removed by employing a wet etching method to remove the surface layer, along with the precursors, thereby returning the optic to a pristine condition. Results of multiple exposure/etch cycles can be seen in Fig. 13 where again damage density from each exposure is normalized to that observed on the first exposure.

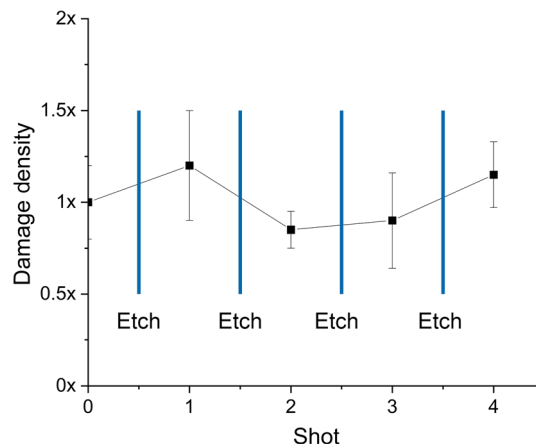


**Fig. 13** Damage density measurements for multiple subsequent exposures of a single sample when interspersed with wet etch processing.

## 4 Discussion/Conclusion

In this work, we have shown that 351-nm exposure of fused-silica surfaces in a vacuum with fluences as low as 12 J/cm<sup>2</sup> generate additional precursors even in regions not exposed to laser fluence. The generation of precursors is not dependent on laser spot size though the rate of precursor generation is affected by the size of the region exposed. We hypothesize that these precursors are particles condensed from SiO<sub>x</sub> vaporized by the laser and accumulate on successive exposures resulting in increased damage site density when exposed with fluences above 20 J/cm<sup>2</sup>. Our observations indicate that these precursors are generated even without the formation of classical damage. The effect of these precursors can be mitigated by physically shielding surface regions from deposition, limiting fluences below the damage threshold of these precursors, or by etching the surface after each exposure to remove them.

## Acknowledgments

This work was performed under the auspices of the U.S. Department of Energy by Lawrence Livermore National Laboratory under Contract No. DE-AC52-07NA27344; Lawrence Livermore National Security, LLC. Portions of this work are included in Proc. SPIE 11173, Laser-induced Damage in Optical Materials 2019, 111730X (20 November 2019).

## References

1. T. I. Suratwala et al., "HF-based etching processes for improving laser damage resistance of fused silica optical surfaces," *J. Am. Ceram. Soc.* **94**(2), 416–428 (2011).
2. T. I. Suratwala, M. D. Feit, and W. A. Steele, "Toward deterministic material removal and surface figure during fused silica pad polishing," *J. Am. Ceram. Soc.* **93**(5), 1326–1340 (2010).
3. T. Suratwala et al., "Sub-surface mechanical damage distributions during grinding of fused silica," *J. Non-Cryst. Solids* **352**(52–54), 5601–5617 (2006).
4. T. Suratwala et al., "Effect of rogue particles on the sub-surface damage of fused silica during grinding/polishing," *J. Non-Cryst. Solids* **354**(18), 2023–2037 (2008).
5. T. Suratwala et al., "Convergent polishing: a simple, rapid, full aperture polishing process of high quality optical flats and spheres," *J. Visualized Exp.* (94), 51965 (2014).
6. J. Hue et al., "R-on-1 automatic mapping: a new tool for laser damage testing," *Proc. SPIE* **2714**, 90–101 (1996).
7. D. Cross and C. W. Carr, "OSL: a laser damage facility," Lawrence Livermore National Laboratory (2020).
8. C. W. Carr et al., "Techniques for qualitative and quantitative measurement of aspects of laser-induced damage important for laser beam propagation," *Meas. Sci. Technol.* **17**(7), 1958–1962 (2006).
9. R. N. Raman et al., "Fate of nanosecond-pulsed 351 nm laser-ejected glass contaminants on fused silica under subsequent laser exposure," *Proc. SPIE* **10805**, 108051L (2018).
10. R. Q. Shen et al., "Ejecta distribution and transport property of fused silica under the laser shock loading," *J. Appl. Phys.* **127**(24), 245114 (2020).
11. C. W. Carr, J. B. Trenholme, and M. L. Spaeth, "Effect of temporal pulse shape on optical damage," *Appl. Phys. Lett.* **90**(4), 041110 (2007).
12. C. W. Carr, J. D. Bude, and P. DeMange, "Laser-supported solid-state absorption fronts in silica," *Phys. Rev. B* **82**(18), 184304 (2010).
13. C. Carr et al., "Using shaped pulses to probe energy deposition during laser-induced damage of SiO<sub>2</sub> surfaces," *Proc. SPIE* **7132**, 71321C (2008).
14. S. Z. Xu et al., "Effect of UV laser conditioning on fused silica in vacuum," *Opt. Mater.* **31**(6), 1013–1016 (2009).
15. L. Lamaignere et al., "An accurate, repeatable, and well characterized measurement of laser damage density of optical materials," *Rev. Sci. Instrum.* **78**(10), 103105 (2007).
16. L. Lamaignère et al., "Damage probability versus damage density: analysis from tests using small beams versus large beams," *Proc. SPIE* **11514**, 115140E (2020).



17. M. Runkel and M. C. Nostrand, "An overview of raster scanning for ICF-class laser optics," *Proc. SPIE* **4932**, 136–146 (2003).
18. J. Y. Natoli et al., "Influence of the test parameters on LIDT determination for single and multiple laser irradiations in optical components in nanosecond regime," *Proc. SPIE* **8786**, 878618 (2013).
19. M. Thomas, "New laser-damage evaluation techniques boost testing capabilities," *Laser Focus World* **53**(5), 27 (2017).
20. C. Grigoriu et al., "Study of Si/SiO<sub>2</sub> nanoparticles produced by laser ablation," *Proc. SPIE* **6195**, 61951A (2006).
21. S. G. Demos, C. W. Carr, and D. A. Cross, "Mechanisms of surface contamination in fused silica by means of laser-induced electrostatic effects," *Opt. Lett.* **42**(13), 2643–2646 (2017).
22. C. H. Li et al., "Laser-irradiation-driven formation of oxygen-related defects and performance degradation in fused silica with nanosecond pulsed laser at 355 nm," *Opt. Laser Technol.* **111**, 727–733 (2019).
23. J. Bude et al., "High fluence laser damage precursors and their mitigation in fused silica," *Opt. Express* **22**(5), 5839–5851 (2014).

**David A. Cross** has been at Lawrence Livermore National Laboratory (LLNL) for the last 15 years and is currently a member of the Damage and Mitigation Science and Technology group for Optics and Materials Science and Technology (OMST) in the NIF and Photon Science Directorate. He attended graduate studies in the field of solid-state physics through the University of California.

**Christopher Wren Carr** has been at LLNL for the last 20 years and is currently the Damage and Mitigation Science and Technology group leader for OMST in the NIF and Photon Science Directorate. He earned his PhD in physics with a specialty in laser-induced damage through the University of California while working on site at LLNL.